

Original Research Article

Computer Aided Static Analysis of Frame and Theoretical Heat Conduction Model for Soya Milk Batch Pasteurizer

Christian Emeka Okafor^{1*}, Efosa Michael Emumwen¹, Samuel Ogbonna Enibe¹, Anthony O. Onokwai²¹Department of Mechanical Engineering, Nnamdi Azikiwe University, Awka, Nigeria²Department of Mechanical Engineering, Landmark University, Omu-Aran, Kwara State, Nigeria

*Corresponding author

Christian Emeka Okafor

Email: ce.okafor@unizik.edu.ng

Abstract: This study covers development of batch (holding) pasteurization equipment, in this method every milk particle is heated to at least 63°C and held for at least 30 minutes. The frame analysis was performed using computer aided design simulation software. The frame parts were modelled and assembled before being exported to the frame simulation environment to check the strength and the level of deformation on the frame. Material indices were derived for energy efficient soya milk batch pasteurizer to determine materials that can resist yielding and rusty condition when exposed to various working environment. Based on the material indices derived, CES software 2013 was used to generate graphs showing materials with adequate thermal conductivity, thermal diffusivity, specific heat capacity, density, yield strength and cost property. Considering the performance criterion, stainless steel and low carbon steel was favoured. The maximum von misses stress on the frame is 102.7Mpa, this value is less than the yield strength of the material of 322.5. Analysis of Variance for heat flow (Q) was carried out and the "Pred R-Squared" of 97.55% is in reasonable agreement with the "Adj R-Squared" of 99.46%. The response surface models developed represents the relationship between the response variable and predictor variables involving the quadric and interaction terms. The model showed that the heat flow (Q) decreases as insulation thickness of the side walls (X_1) increases and that area of the walls (X_2) has least influence on the variability of heat flow, it also indicates that the heat flow is optimum when insulation thickness of the side wall (X_1) = 50mm, Area of the side wall (X_2) = 12780 mm², and insulation thickness of the lid cover (X_3) = 45mm. Above all, the result of the frame after FEA reveals the suitability and stability of the materials and the dimensions for the intended purpose.

Keywords: Batch Pasteurizer, theoretical model, frame analysis, soya milk, material selection.

INTRODUCTION

Milk borne diseases in developing countries leads to millions of deaths and billions of illnesses annually. Milk disinfection is one of several interventions that can improve public health, especially if part of a broad program that considers all disease transmission routes and sustainable involves the community [1, 2]. Pasteurization process has become the most important process especially in dairy and beverage industries, the aim of the process is to preserve the product quality and to extend the shelf life of product [3]. Pasteurization therefore is a relatively mild heat treatment in which food is heated to <100°C. As a unit operation in food processing it can be used to destroys enzymes and relatively heat sensitive microorganisms. In this regard it is used to extend shelf life by several days, e.g. milk or months, e.g. bottled fruit [4]. The milk and its products are fundamental in

human nutrition. It can be used as an important part of his diet throughout life. The milk is a perishable foodstuff because it is an excellent medium for the growth of microorganisms which cause spoilage. Heating milk to a specific temperature for a specific period of time, lead to killing harmful microorganisms [2].

Franco *et al.* [6] have designed a system for pasteurizing 10 l of milk in about 1 hour. Zahira *et al.* [5] fabricated a solar milk pasteurizer having inner box volume of (52.5×24×36) cm covered on both sides with aluminum foil. Atia, Mostafa, Abdel-Salam and El-Nono [2] conducted a design and performance analysis of pasteurization system that is based on the solar energy as a thermal source for pasteurizing the milk has been done. The pasteurization temperatures were 63 and 72°C. The solar milk pasteurizer, during September,

October and November 2009, attained pasteurization temperatures in 3 to 19 minutes depending on the solar radiation, and the desired temperature for pasteurization. The average daily maximum amount of solar-pasteurized milk was 73.9 l at 63°C, while the minimum was 37.3 l at 72°C. The change in intensity of solar radiation had a direct impact on solar milk pasteurizer.

Wayua, Okoth and Wangoh [7] developed an artificial neural network model to predict milk temperature of a locally fabricated solar milk pasteuriser, based on measures of error deviation from experimental data. The neural network predictions agreed well with experimental values with mean squared error, mean relative error and correlation coefficient of determination (R^2) of 5.22°C, 3.71% and 0.89, respectively. Wayua, Okoth and Wangoh [8] designed and assessed the performance of a flat-plate solar milk pasteurizer for arid pastoral areas of Kenya. The solar milk pasteurizer consist of flat-plate water-heating collector and a 1.5-mm thick stainless steel cylindrical milk vat was designed and tested in an arid pastoral area of northern Kenya. The milk vat had a capacity of 80 L and a 50-mm wide hot water jacket insulated with 38-mm thick fiberglass.

Rehman and Al-Hilphy [9] designed and manufactured a non thermal milk pasteurizer using electrical field, the study focused on applying different electrical fields in milk pasteurization as a non thermal treatment. Rabab, Hafiz, Nasir and Muhammad [1] carried out fabrication and performance study of a solar milk pasteurizer. This experimentation was done on temperature ranging from 65°C to 75°C. Mokhtar [3] developed an empirical model of coconut milk pasteurization process using plate heat exchanger. The model was developed based on experimental data and represented in first order plus time delay (FOPTD) model. Overall, the obtained model gave good agreement with experimental data in validation result with maximum error is $\pm 5\%$. The validation result showed that this model is suitable for use in control strategy for the further study.

There is a dearth of theoretical models for soya milk pasteurizer design, although Mukhopadhaya and Raju [10] tried to develop a theoretical heat conduction model for cold storage using Taguchi methodology, the limitations of Taguchi method in accounting for interaction and second order effects of factors requires application of a more robust response surface method. Also there is need to ensure suitability and stability of the fabrication materials for the intended purpose.

MATERIAL AND METHODS

This study covers development of batch (holding) pasteurization equipment, in this method every milk particle is heated to at least 63°C and held for at least 30 minutes. The outer box has volume (639×659×582) mm³. The frame analysis was performed using computer aided design simulation software. The frame parts were modelled and assembled before being exported to the frame simulation environment to check the strength and the level of deformation on the frame [11]. The values of loads used for the analysis were obtained from i-properties tab of Autodesk Inventor software and is as summarized in table 1, this values are the sum of individual components of the machine resting on different sections of the machine. The weights were assumed to be evenly distributed on the frame by sections. Fixed constraints were used in constraining the base of the frame to ensure stability before performing the frame analysis simulation. The frame is the structural part that supports the entire load of the machine. It is subjected to the weight of the other components of the machine. Hence the frame is subjected to compressive forces. The material used for frames should be of high rigidity and toughness. This will enhance the stability of the machine. The frame will be tested for static strength. The weight acting on the frame as shown in table 1 was assumed to be evenly distributed on the frame by sections. Fixed constraints were used in constraining the base of the frame. The materials used for the components were specified in the solid model before extracting the various masses of the section. The volume of the inner chamber was used as the control volume to get the maximum mass of water the machine can contain.

Material selection

Desirability factors for selection based on strength and cost of candidate materials are differently expressed by Crawford, 1998 and Ashby, 2003. When the pasteurizer is heated, the internal temperature rises quickly from ambient, T_o , to the operating temperature T_i , where it is held for the pasteurization time t (say 30min). The energy consumed in heating time (t) has two contributions. The first is the heat conducted out; at steady state the heat loss by conduction Q_1 per unit area is given by the first law of heat flow, if held for time t is

$$Q_1 = -\lambda \frac{dT}{dx} t = \lambda \frac{(T_i - T_o)}{w} t \tag{1}$$

While the second contribution is the heat absorbed by the pasteurizer wall in raising it to T_i per unit area it is

$$Q_2 = C_p \rho w \left(\frac{T_i - T_o}{2} \right) \tag{2}$$

Where λ is the thermal conductivity, $\frac{dT}{dx}$ is the temperature gradient, C_p is the specific heat of the wall material, ρ is the density and w is the insulation wall thickness. The total energy consumed per unit area is the sum of these two

$$Q = Q_1 + Q_2 = \lambda \frac{(T_i - T_o)}{w} t + C_p \rho w \left(\frac{T_i - T_o}{2} \right) \quad (3)$$

Thus to determine the optimum thickness, we differentiate equation (2) with respect to wall thickness w and equating the result to zero, giving

$$w = \left(\frac{2 \lambda t}{C_p \rho} \right)^{1/2} = (2at)^{1/2} \quad (4)$$

Where $a = \frac{\lambda}{C_p \rho}$ is the thermal diffusivity. The quantity $(2at)^{1/2}$ has dimensions of length and is a measure of the distance heat can diffuse in time $t = 30$ min. Eliminating w we have

$$Q = (T_i - T_o)(2t)^{1/2} (\lambda C_p \rho)^{1/2} \quad (5)$$

Q is minimised by choosing a material with a low value of the quantity $(\lambda C_p \rho)^{1/2}$ that is by maximizing

$$M_1 = (\lambda C_p \rho)^{1/2} = \frac{a^{1/2}}{\lambda} \quad (6)$$

However, before accepting any candidate material we must check, by evaluating equation 4 to determine how thick the wall made from it will be. Also Minimize cost per kg of the material

$$M_2 = \frac{\lambda \sigma_y^2}{C_m \rho} \quad (7)$$

Where ρ = density of tube material, C_m = cost per kg of the material, σ_y is now raised to the power of 2 because the weight depends on wall thickness as well as density and wall thickness varies as $\frac{1}{\sigma_y}$. The material with the highest M is usually chosen as a candidate material. The acceptable wall thickness is calculated from equation 4 at a milk pasteurizing temperatures of 63°C for 30 min (low temperature long time LTLT) and Heat transfer is calculated by using Fourier's law-

$$\text{Heat flow}(Q) = \frac{K \times A \times (T_i - T_o)}{X} \quad (8)$$

Where, K = thermal conductivity of insulating material =0.04 W/mk , A = area TD= temperature difference. X = insulation thickness.

Theoretical Model development

The fresh-milk pasteurizer has a design capacity of 25 litres. It is insulated by fibreglass. Three control parameters, viz. insulation thickness of the side walls (X_1), area of the walls (X_2), Insulation thickness of the lid cover (X_3) taken as predictor variables and heat flow (Q) taken as response variable. Table 1 shows all the control parameters and their levels.

The temperature inside the pasteurizer is taken as 63°C and assume that it is constant throughout the chamber. RSM uses many experiments to reach optimum and at optimum the appropriate model is nonlinear regression model. The general polynomial model to detect nonlinearity and second order effects is expressed as

$$\hat{Y} = \beta_0 + \sum_{i=1}^k \beta_i X_i + \sum_{i=1}^k \beta_{ii} X_i^2 + \sum_{i=1}^{k-1} \sum_{j=2}^k \beta_{ij} + \epsilon \quad (9)$$

Table 1: control parameters and their levels

Factors	Unit	Levels	
		#1	#2
Insulation thickness of the side wall (X_1)	mm	20	50
Area of the side wall (X_2)	mm ²	12780	31450
Insulation thickness of the lid cover (X_3)	mm	25	45

Table 2: Central composite design (CCD) matrix for heat flow (Q)

Std Order	Run Order	X_1 (mm)	X_2 (mm ²)	X_3 (mm)	Heat flow (Q) (W)
20	1	35	22115	35	909.8743
3	2	20	31450	25	2012.8
8	3	50	31450	45	953.4316
10	4	60.22689	22115	35	668.8363

2	5	50	12780	25	490.752
9	6	9.773108	22115	35	1422.532
11	7	35	6415.464	35	263.9505
15	8	35	22115	35	909.8743
18	9	35	22115	35	909.8743
1	10	20	12780	25	817.92
4	11	50	31450	25	1207.68
6	12	50	12780	45	387.4358
14	13	35	22115	51.81793	733.6181
12	14	35	37814.54	35	1555.798
13	15	35	22115	18.18207	1197.607
17	16	35	22115	35	909.8743
7	17	20	31450	45	1393.477
19	18	35	22115	35	909.8743
5	19	20	12780	45	566.2523
16	20	35	22115	35	909.8743

RESULTS AND DISCUSSIONS

Material selection

Having carried out a search for materials that can suite the in-service condition of fresh-milk pasteurizer, the following materials presented in Table 3

met the search criteria as potential materials that can be used for the aforementioned application. Each of the parameter plotted for in Figure 1 and 2 was based on the moderate temperature condition the fresh-milk pasteurizer is exposed to, during operation.

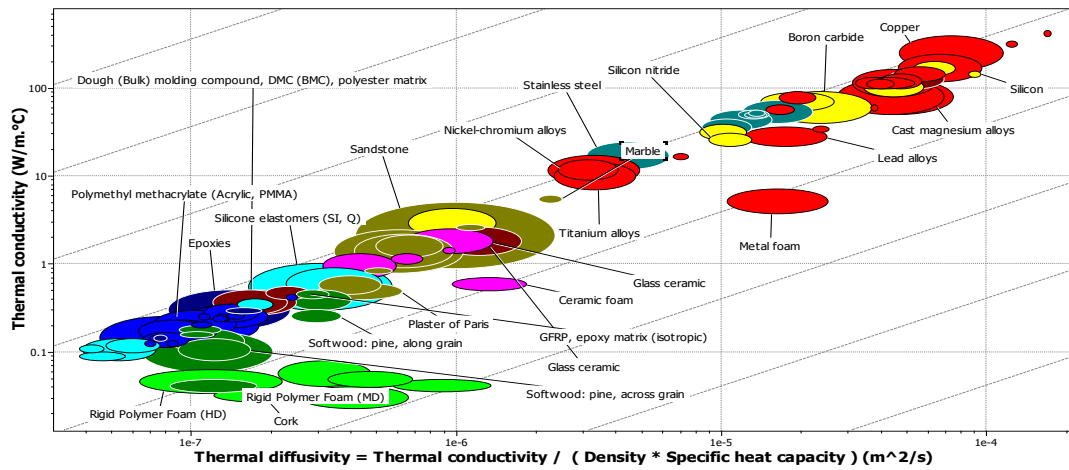


Fig-1: λ-a chart for energy-efficient pasteurizer

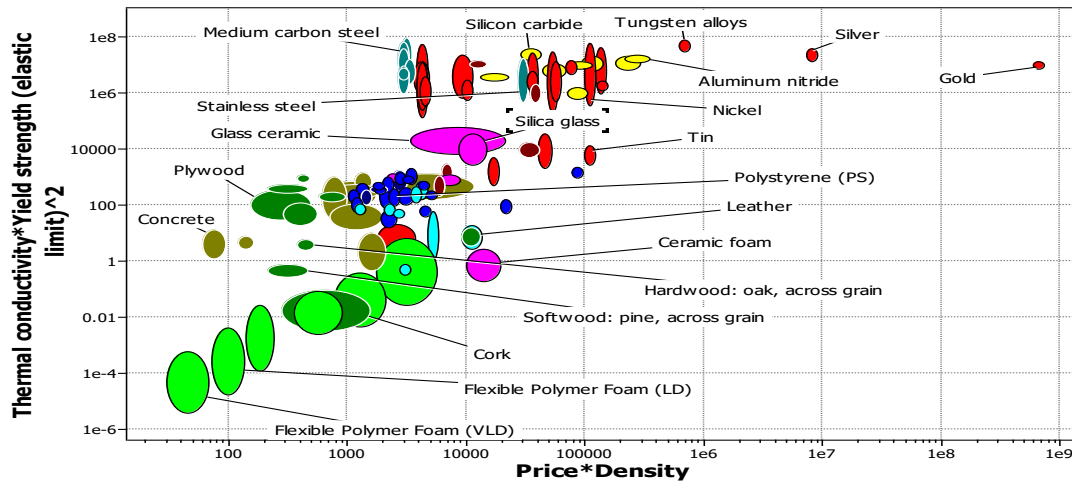


Fig-2: material selection chart for energy-efficient pasteurizer based on cost

Figure 1 shows the result of materials obtained when thermal conductivity is plotted against thermal diffusivity and Stainless steel and Low carbon steel

were in that category while Figure 2 shows the results obtained when material performance index is based on cost.

Table 3: Candidate materials for energy-efficient pasteurizer

Material	Density (kg/m ³) (ρ)	Price (387.09 GBP/kg) (C_m)	Thermal conductivity (W/m.°C) (λ)	Specific heat capacity (J/kg.°C) (C_p)	Yield strength (MPa) (σ_y)	Thermal diffusivity (a) = $\frac{\lambda}{C_p\rho}$	$w = (2at)^{1/2}$	$M_2 = \frac{\lambda\sigma_y^2}{C_m\rho}$	$M_1 = \frac{a^{1/2}}{\lambda}$
Stainless steel	7.85E3	3.815	18	490	585	4.68E-06	0.016756	3295.29	0.00012
Low carbon steel	7.84E3	0.367	51.5	482.5	322.5	1.36E-05	0.028581	30248.46	7.16E-05
GFRP epoxy matrix(isotropic)	1.86E3	18.5	0.475	1.1e3	151	2.32E-07	0.003732	0.53221	0.001014
Glass ceramic	2.6E3	4.065	1.92	750	119.75	9.85E-07	0.007686	9.030888	0.000517
Marble	2.79E3	0.457	5.5	870	8	2.27E-06	0.01166	0.885334	0.000274

Results of static frame Analysis

Properties of the two materials selected were used to implement static analysis of frame, while stainless steel was used in design of pasteurizing

chamber, low carbon steel was used for the design of the base. Table 4 shows the frame weight distribution while table 5 indicates reaction force and reaction moment distributions.

Table 4: Frame weight distribution table

Section	Load (kg)	Weight (N)
Casing	54.34	543.4
Insulation material	84.34	843.4
Piping accessories	2.368	23.68
Water content	68.92	689.2
Total	209.97	2099.7

Table 5: Reaction force and reaction moment distributions

Constraint Name	Reaction Force		Reaction Moment	
	Magnitude	Component (Fx, Fy, Fz)	Magnitude	Component (Mx, My, Mz)
Fixed constraint: 1	577.808N	20.851 N	2989.333 N mm	2108.541 N mm
		577.052 N		1.158 N mm
		-20.939 N		2114.768 N mm
Fixed constraint: 2	579.477 N	-21.389 N	2712.586 N mm	1956.382 N mm
		578.725 N		6.652 N mm
		-20.352 N		-1879.002 N mm
Fixed constraint: 3	577.507 N	-19.732 N	2942.638 N mm	-2077.814 N mm
		576.830 N		1.164 N mm
		19.821 N		-2083.700 N mm
Fixed constraint: 4	579.477 N	20.270 N	2172.795 N mm	-1874.326 N mm
		578.724 N		-8.418 N mm
		21.470N		1961.14 5 N mm

The red colour on the colour bar signifies area of high stress concentration while the blue part signifies area of less stress concentration for figure 4 and 5. Von misses' failure criterion is used in evaluating the frame. According to the failure criterion, material will fail if the maximum value of von misses stress induced in the material is more than the yield strength of the material. The maximum von misses stress on figure 4 is

102.7Mpa, this value is less than the yield strength of the material of 585MPa and 322.5MPa for both stainless steel and low carbon steel respectively. Thus the frame is considered to be stable. The maximum factor of safety for the frame is 15. The red colour on the colour bar signifies area of high stress concentration while the blue part signifies area of less stress concentration for figure 3 and 4.

Table 6: Static Result Summary

Name	Minimum	Maximum
Displacement	0.00mm	0.036
Forces	Fx	-272.892 N
	Fy	-271.873
	Fz	-66.539 N
Moments	Mx	-14790.540Nmm
	My	-18667.390Nmm
	Mz	-985.503N
Normal Stresses	Smax	-1.277 Mpa
	Smin	-14.207 Mpa
	Smax(Mx)	0.000 Mpa
	Smin(Mx)	-8.728 Mpa
	Smax(MY)	0.000 Mpa
	Smin (My)	-8.638 Mpa
	Saxial	-1.295 Mpa
Shear Stresses	Tx	-1.638 Mpa
	Ty	1.645 Mpa
Torsional stresses	T	-0. 736 Mpa

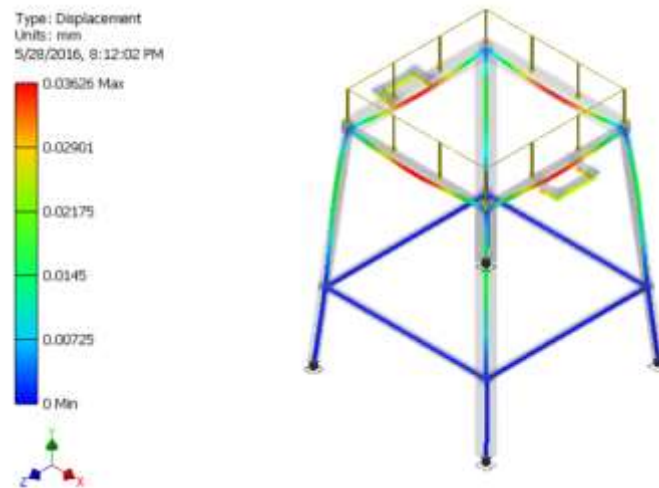


Fig-3: Displacement diagram of the frame

Figure 3 shows displacement diagram of the frame in all load cases while table 4 shows the displacement values from the range of frames analysed and the optimised responses. The optimised values show a considerable improvement over the best of

the existing frames, with a 13% increase in vertical displacement and 15% decrease in lateral displacement when compared to the best of the analysed frames.

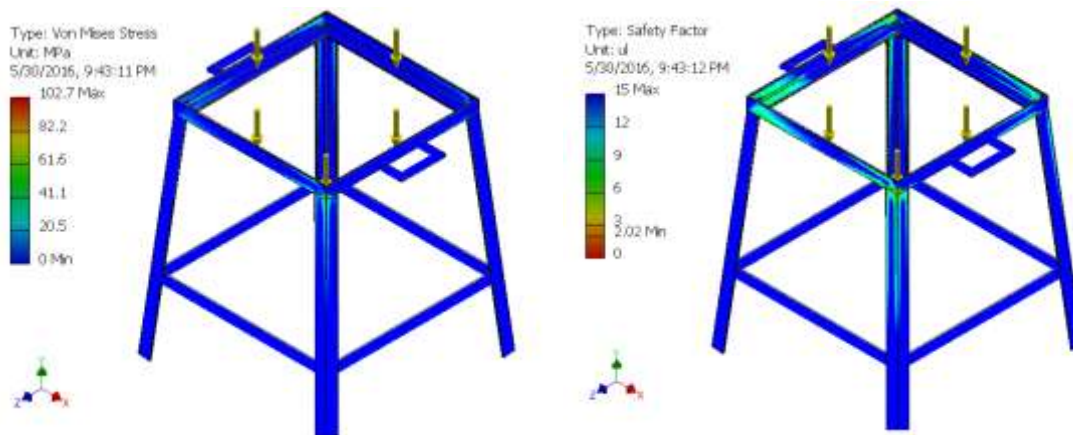


Fig-4: FEA Analysis results showing Von Mises stress and factor of safety of the frame

From the results of FEA, it is apparent that the stresses induced in the frame of pasteurizer is least and the factor of safety is also well above the limit. The use of ANSYS software makes the process of calculation

fast and several iterations are permissible to arrive at the best possible results. The results are relevant provided the assumptions and boundary conditions are perfect.



Fig-5: Soya Milk Batch Pasteurizer CAD Model

Response surface results

From table 7, the R-Squared value indicates that 97.55% variation in heat flow was due to independent Variable, only about 2.45 % cannot be

explained by the model, so it is concluded that the theoretical model is adequate to describe the flow of heat by response surface.

Table 7: Analysis of Variance for heat flow (Q)

Source	DF	Seq SS	Adj SS	Adj MS	F	P
Regression	9	3332073	3332073	370230	386.81	0.000
Linear	3	3159796	3159796	1053265	1100.42	0.000
X_1	1	667255	667255	667255	697.13	0.000
X_2	1	2197038	2197038	2197038	2295.41	0.000
X_3	1	295502	295502	295502	308.73	0.000
Square	3	37411	37411	12470	13.03	0.001
X_1^2	1	31635	33554	33554	35.06	0.000
X_2^2	1	44	1	1	0.00	0.977
X_3^2	1	5732	5732	5732	5.99	0.034
Interaction	3	134866	134866	44955	46.97	0.000
$X_1 * X_2$	1	68299	68299	68299	71.36	0.000
$X_1 * X_3$	1	32951	32951	32951	34.43	0.000
$X_2 * X_3$	1	33617	33617	33617	35.12	0.000
Residual Error	10	9571	9571	957		
Lack-of-Fit	5	9571	9571	1914		
Pure Error	5	0	0	0		
Total	19	3341644				

S = 30.9378, PRESS = 81947.8, R-Sq = 99.71%, R-Sq(pred) = 97.55% and R-Sq(adj) = 99.46%.

From table 7, the "Pred R-Squared" of 97.55% is in reasonable agreement with the "Adj R-Squared" of 99.46%. The response surface models in terms of actual factors is in equations (10). It represents the relationship

between the response variable and predictor variables involving the linear, quadric, and interaction terms. The models show that the insulation thickness of the side walls (X_1) has the highest effect on the heat flow

response. Also interaction effects are shown to be depicted. significant; both main and high order effects were also

$$\text{Heat flow}(Q) = 974.456 - 30.1300 X_1 + 0.0902460 X_2 - 28.2880 X_3 + 0.214457X_1^2 + 2.71641E - 09X_2^2 + 0.199432 X_3^2 - 6.59865E - 04 X_1X_2 + 0.427855 X_1X_3 - 6.94413E - 04 X_2X_3 \quad (10)$$

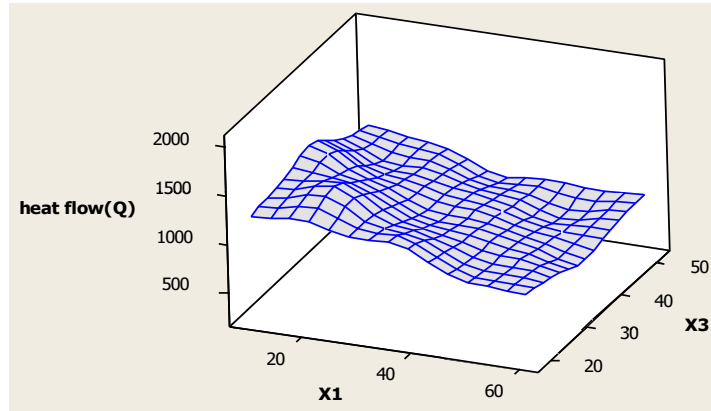


Fig-6: 3-D surface plot of variation of heat flow with insulation thickness of the side walls (X₁) and Insulation thickness of the lid cover (X₃)

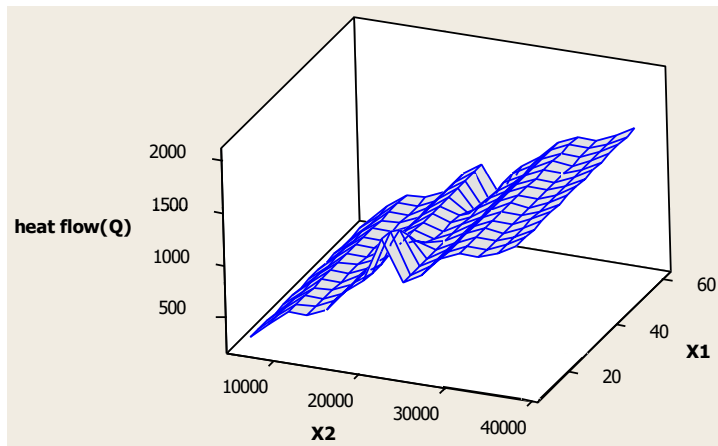


Fig-7: 3-D surface plot of variation of heat flow with insulation thickness of the side walls (X₁), area of the walls (X₂)

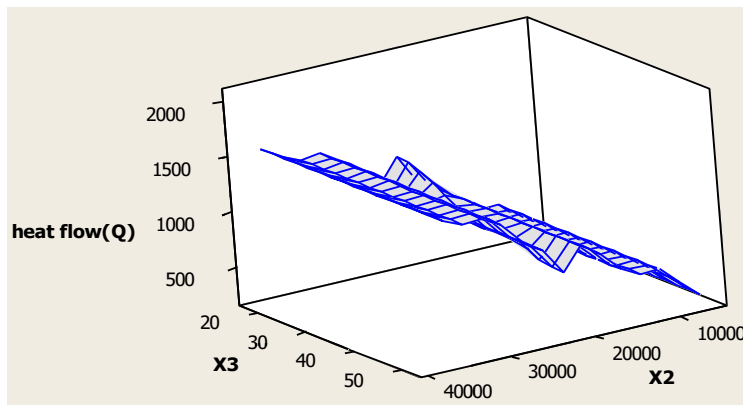


Fig-8: 3-D surface plot of variation of heat flow with area of the walls (X₂), Insulation thickness of the lid cover (X₃)

Figure 3-5 show that the heat flow decreases as insulation thickness of the side walls (X_1) increases and that area of the walls (X_2) has least influence on the variability of heat flow, it also indicates that the heat flow is optimum when insulation thickness of the side wall (X_1) = 50mm, Area of the side wall (X_2) = 12780 mm², and insulation thickness of the lid cover (X_3) = 45mm.

CONCLUSION AND RECOMMENDATION

The conceptual design and computer aided static analysis of frame and theoretical heat conduction model for soya milk batch pasteurizer has been presented. The modelling was done with CAD and DOE software; hence Finite Element Analysis was used to evaluate the stress values on the machine structure by replacing infinite atoms with finite nodes and the bonds replaced by elements. Material selection considerations ensured that appropriate materials is used in the design. For fresh-milk pasteurizer having design capacity of 25 litres, it is recommended that insulation thickness of the side wall should be set at 50 mm while the area of the side wall should be 12780 mm², and 45 mm insulation thickness is recommended for the lid cover.

REFERENCES

1. Rabab Z, Hafiz A, Nasir A and Muhammad A. Fabrication and performance study of a solar milk pasteurizer. *Pak. J. Agri. Sci.* 2009;46(2):162-170.
2. Atia MF, Mostafa MM, Abdel-Salam MF, El-Nono MA. Solar Energy Utilization for Milk Pasteurization. Available from: Mohamed Fathey Mohamed Atia. Retrieved on: 09 September 2016.
3. Mokhtar WMFW. Empirical Modelling of Pasteurization Process Using Plate Heat Exchanger. *International Journal of Engineering Research & Technology.* 2012;1(3):1-5.
4. Safefood. Thermal Processing of Food. Safefood 360, Inc. Professional Whitepapers Series, 2014.
5. Zahira R, Hafiz A, Nasir A, Muhammad A, Zia-ul-Haq. Fabrication and performance study of a solar milk pasteurizer, *J. Agri. Sci.* 2009;46(2).
6. Franco J, Saravia L, Javi V, Ricardo C, Carlos F. Pasteurization of goat milk using a low cost solar concentrator, *Solar Energy J.* 2007. doi:10.1016/j.solener.2007.10.011, USA.
7. Wayua FO, Okoth MW, Wangoh J. Modelling of a locally fabricated flat-plate solar milk pasteuriser using artificial neural network. *African Journal of Agricultural Research.* 2013;8(9):741-749.
8. Wayua FO, Okoth MW, Wangoh J. Design and performance assessment of a flat-plate solar milk pasteurizer for arid pastoral areas of Kenya. *Journal of Food Processing and Preservation.* 2011. doi:10.1111/j.1745-4549.2011.00628.x
9. Rehman A, Al-Hilphy S. Designing and manufacturing of a non thermal milk pasteurizer using electrical field. *American Journal of Agricultural and Biological Sciences.* 2013;8(3):204-211.
10. Mukhopadhaya N, Raju D. Theoretical heat conduction model development of a Cold storage using Taguchi Methodology. *International Journal of Modern Engineering Research (IJMER).* 2014;4(6):77-82.
11. Metu CS, Enibe SO, Ulasi TS. Conceptual Design and Computer Aided Static Analysis of Frame and Plates of a Continuous Process Breadfruit De-Pulping Machine. *American Journal of Mechanical Engineering and Automation.* 2016;3(3):22-28.
12. Robinson K. Dairy microbiology handbook, Wiley and Sons Inc., New York, USA. 2002;(3):31-35.
13. Sigley JE, Mischke CR. Standard Handbook of Machine Design, Second Edition. Mc Graw- Hill Publications, 1996.